ELSEVIER

Journal of Power Sources 111 (2002) 104–108

JOURNAL OF POWER SOURCES

www.elsevier.com/locate/jpowsour

Lithium insertion into $Cr_2(So_4)_3$ frameworks: variation of electrochemical behavior with cation substitution and nature of polyanion

M. Manickam, M. Takata*

Department of Electrical Engineering, Nagaoka University of Technology 1603-1 Kamitomioka, Nagaoka 940-2188, Niigata, Japan

Received 25 April 2002; accepted 3 May 2002

Abstract

Electrochemical insertion of lithium into the $Cr_2(SO_4)_3$ framework was carried out in a ''Li|$LiClO_4$:EC–PC (3:1)|cathode'' cylindrical cell (EC: ethylene carbonate, PC: propylene carbonate). Preliminary electrochemical data revealed that the $Cr_2(SO_4)_3$ sample exhibit poor performance compared to the cation- and polyanion-substituted samples. Depending on the cation (Nb) substitution and the nature of the polyanion (XO_4) (X = P and S): (a) a clear dependence of the shape of the discharge curve versus capacity; and (b) an enhancement of voltage and capacity rate have been obtained and their difference is discussed in terms of redox potential. The cathodes with Nb substitution and polyanion having $(PO_4)^{3-}$ are more tolerant to repeated lithium insertion and extraction than a standard $Cr_2(SO_4)_3$ framework electrode in spite of a small reduction in the open-circuit voltage. The improvement in cycling performance is attributed to the presence of Nb cations that enhance the stability of the octahedral sites in the structure.

Keywords: Polyanion; Lithium insertion; Redox potential; Battery

1. Introduction

The enormous demand for portable electronic devices, such as laptop computers and mobile telephones, has created increasing scientific and technological interest in the development of inexpensive and environmentally friendly rechargeable lithium batteries. In this regard, spinel $LiMn_2O_4$ [1,2] and layered $LiCoO_2$ [3,4] have been investigated intensively over the years. Recently, cost, environmental and shelf-life considerations have prompted the search for alternative cathode systems, among which are NASICON framework structures utilizing the transition metal redox potential and tetrahedral polyanions $(XO_4)^{2-}$ or $(XO_4)^{3-}$ with X = Mo, W or P [5–8]. The Na^+ superionic conductor $Na_3Zr_2Si_2PO_{12}$, NASICON, belongs to a class of NZP ($NaZr_2(PO_4)_3$) phases with the general formula $Na_{1+x}Zr_2P_{3-x}Si_xO_{12}$ [9,10]. Several oxides of the general formula $A_nM_2(XO_4)_3$ crystallize with $M_2(XO_4)_3$ frameworks consisting of a three-dimensional network of XO_4 tetrahedra sharing corners with MO_6 octahedra and a three-dimensional linked interstitial space occupied by A-cations [11]. Initial investigations have used lithium as A-cation. A few $M_2(XO_4)_3$ frameworks are stable in the complete absence of A-cation [12]; these include molybdates and tungstates of the trivalent M = Fe, Cr and Sc [7]. The availability of a framework not only supports fast lithium ion conduction but also provides transition metal ions having an accessible redox potential, thereby paving the way for the use of these materials as an electrode for secondary batteries. Lithium can be inserted electrochemically into the host, though the metal atom present in the structure is reducible by elemental lithium. This, however, usually occurs when the metal atom in the host lattice exhibits a variable valence [8,12].

We undertook systematic investigations of lithium insertion into different polyanion structures ($(SO_4)^{2-}$ and $(PO_4)^{3-}$) operating at different transition metal redox potentials (Cr^{3+}/Cr^{2+}, Nb^{5+}/Nb^{4+} and Nb^{4+}/Nb^{3+}). Of particular interest are the tuning of the transition metal redox potential, which depends on the nature of the polyanion and the identification of new cathode materials operating at the Nb^{5+}/Nb^{4+} redox potential. Among these, $Li_xCr_{0.5}Nb_{1.5}(PO_4)_3$ with a closed-circuit voltage at 2.3 V versus lithium, presents better performance [13].

In this paper, we describe the electrochemical properties of $Cr_2(SO_4)_3$ framework structures. Depending on the cation substitution and the nature of the polyanion group (XO_4) (X = P and S), three discharge curve profiles have been

* Corresponding author. Tel.: +81-258-47-9509; fax: +81-258-47-3604.
E-mail address: takata@vos.nagaokaut.ac.jp (M. Takata).

0378-7753/02/$ – see front matter
PII: S0378-7753(02)00266-5

obtained and their difference is discussed. Moreover, the open-circuit voltage (V_{oc}) of this framework is compared with those of various prototypical intercalation compounds.

2. Experimental

Direct decomposition and solid state reaction in air at 600 °C between intimately mixed Cr_2O_3 (99.9%) and NH_4HSO_4 powder with intermittent grinding led to the formation of $Cr_2(SO_4)_3$.

The cation-substituted compound $Cr_{0.5}Nb_{1.5}(XO_4)_3$ with the polyanion X = S and P, was prepared by solid state reaction in air. Starting materials were Cr_2O_3 (99.9%), Nb_2O_5 (99.9%) and $NH_4H_2XO_4$ powder. The stoichiometric mixture was mixed thoroughly in a mortar and heated at 200 °C for 12 h to drive off NH_3, H_2O and other gaseous products. The mixture was then heated at 600 °C for 5 h and at 930 °C for 12 h with intermittent grinding. Phase identification and evaluation of the lattice parameters of the products were carried out by powder X-ray diffraction (XRD) using Cu Kα radiation. Electrochemical performance was evaluated with cylindrical test cells. The procedures for the fabrication and the measurement of lithium rechargeable cells are almost the same as those described elsewhere [13,14]. The electrode materials were first mixed with 15 wt.% of acetylene black and with 10 wt.% of PVDF and then pressed. The mixture was ground and then pressed into a disk with a diameter of 10 mm at 78 MPa. All disks (cathodes) were mixed with a binder, without which the disks could not be handled. The thickness of each disk was 1 mm and the weight was about 60 mg. Each disk was dried at 80 °C for 30 min. An electrochemical testing cell was constructed with the disk as the cathode, the lithium foil as the anode and filter paper as the separator. The electrolyte was 1 M $LiClO_4$ in EC–PC 3:1 (v/v) (Tomiyama; EC: ethylene carbonate, PC: propylene carbonate). Cell performance was evaluated galvanostatically at a current density of 0.25 mA/cm^2 with the aid of charge–discharge unit (Hokuto Denko HJ-201B). The cells were first discharged and then charged at constant current density between the potential limit of 1.5 V for discharge and 3.2 V for charge. The potential limits that were used for the Li|$Li_xCr_2(SO_4)_3$ cell alone were 1.3–1.5 V. All electrochemical measurements were carried out in a glove box filled with argon at room temperature.

3. Results and discussion

The XRD pattern of the product $Cr_2(SO_4)_3$, Fig. 1(a), showed that a single-phase compound [15] was obtained with a small amount of Cr_2O_3. On inserting lithium electrochemically into the $Li_xCr_2(SO_4)_3$ sample, the voltage decreases with x, over most of the compositional range ($0 \leq x \leq 1.0$); however, the discharge capacity declines

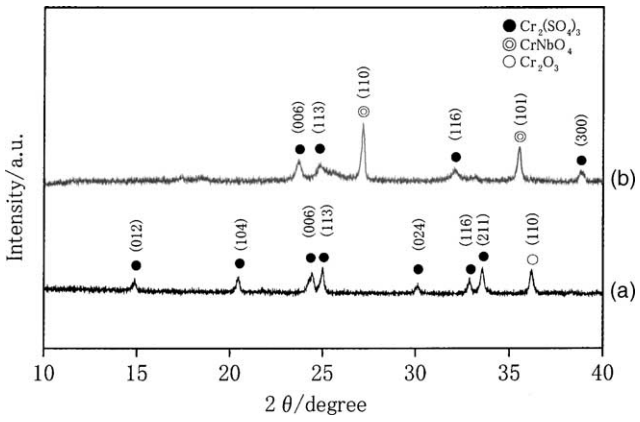

Fig. 1. XRD patterns of: (a) $Cr_2(SO_4)_3$; (b) Nb-substituted $Cr_2(SO_4)$ framework $Cr_{0.5}Nb_{1.5}(SO_4)_3$.

gradually with increasing x values (Fig. 3(a)). At a cut-off voltage of 1.5 V, voltage declines sharply with lithium composition, $x = 0.1$, corresponding to 13 mAh/g. At a cut-off voltage of 1.3 V, lithium insertion into the structure proceeds via a single-phase mechanism in which lithium content is varied continuously [16]. The insertion of lithium into this sample corresponding to a discharge capacity of 50 mAh/g at a cut-off voltage of 1.3 V is attributed to the reduction of Cr^{3+} to Cr^{2+} on the octahedral sites of the NZP structure. When this type of cell at a cut-off voltage of 1.3 V was subsequently discharged (third discharge), as shown in Fig. 4(a) the discharge profile looks alike at the initial stage but the cell had a sharp drop in voltage compared to that of the first discharge and the lithiation process stopped at a minimum of 20 mAh/g. These changes in the voltage on cycling imply that the structure may change via lithiation and delithiation.

The XRD pattern of the cation-substituted product (Fig. 1(b)), shows the presence of a composite of $Cr_{0.5}Nb_{1.5}(SO_4)_3$ and $CrNbO_4$ that has tetragonal symmetry. The diffraction pattern for the cation Nb-substituted product (Fig. 1(b)) indicates retention of the $Cr_2(SO_4)_3$ framework with the shift of the peaks to smaller angles caused by a marginal increase in ionic radii for Nb atoms. Some new peaks reveal the nucleation of a second phase, niobium chromium oxide, as the impurity. The plot of voltage versus discharge capacity for $Li_xCr_2(SO_4)_3$ in Fig. 3(a) is compared with that for the Nb-substituted framework $Li_xCr_{0.5}Nb_{1.5}(SO_4)_3$ (Fig. 3(b)). Two features are observed from these plots: (1) the open-circuit voltage (V_{oc}) for the cell Li|$Li_xCr_{0.5}Nb_{1.5}(SO_4)_3$ at $x = 0$ results in a decrease of 0.2 V, $Cr_2(SO_4)_3$: 3.34 V and $Cr_{0.5}Nb_{1.5}(SO_4)_3$: 3.1 V; (2) the voltage and discharge capacity have been improved much for the Nb-substituted framework at the cut-off voltage of 1.5 V. The first feature can be explained by the fact that apart from the well-known covalency of S–O bonds in the tetrahedra [17], Cr–O bonds are more covalent than Nb–O ones since Cr^{3+} is a smaller and more highly polarized ion than Nb^{3+} (as noted from the IR spectra, not shown

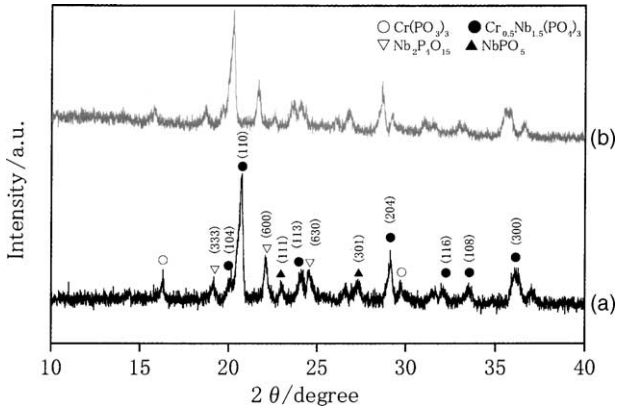

Fig. 2. XRD patterns of $Cr_{0.5}Nb_{1.5}(PO_4)_3$: (a) before Li insertion; (b) after Li insertion.

here); therefore, the open-circuit voltage for $Cr_2(SO_4)_3$ is higher than that for $Cr_{0.5}Nb_{1.5}(SO_4)$. The second feature shows that the substitution of Nb^{3+} for Cr^{3+} leads to a marked increase in voltage during discharge. It is clear that niobium substitution on the polyanion $(SO_4)^{2-}$ affects the electrochemistry of the NZP-type electrode, which can be interpreted in terms of the coordination and reduction state of niobium atoms.

The XRD pattern of the polyanion-substituted sample (X = P) prepared by solid state reaction in air at 930 °C is shown in Fig. 2(a). The lattice parameters of the compound matched with those of the hexagonally-structured $TiNb(PO_4)_3$ powder diffraction file 25-0984. The data reveal that the sample is a multiphase compound with chromium phosphate and niobium phosphate as impurities. Although the compound is a multiphase one, the intercalation reaction still occurs and shows higher capacity and improved cyclability compared to $(SO_4)^{2-}$ polyanion. Depending on the nature of the (XO_4) polyanion, the plot of voltage versus discharge capacity for X = P in Fig. 3(c) is compared with that for X = S in Fig. 3(b). Both modifications of $Cr_{0.5}Nb_{1.5}(XO_4)_3$ (X = P and S) have nearly the same open-circuit voltage. Unlike $(SO_4)_3$, there exists a change in the shape of the discharge curve with two plateau-like regions. The insertion of lithium into the $(PO_4)_3$ framework has two separate intercalation plateau-like regions at 2.3 and 1.6 V for $0 \leq x \leq 1$ and $1 \leq x \leq 2.3$, respectively. The XRD pattern of the lithiated compound (Fig. 2(b)) supports the contention that electrochemical lithiation is involved during the intercalation process. The XRD pattern after lithiation is very similar to that observed before lithiation, except for a limited structure expansion that is revealed by the shift of the peaks to smaller angles. The discharge curve in Fig. 3(c) is characterized by an immediate sharp drop in voltage to 2.5 V, followed by a gradual downward sloping potential over a long period of time until 2.1 V, corresponding to the Nb^{5+}/Nb^{4+} redox couple. Then, again, the sharp drop at 2 V is followed by a gradual change in voltage till 1.5 V, which corresponds to Nb^{4+}/Nb^{3+} redox couple. The

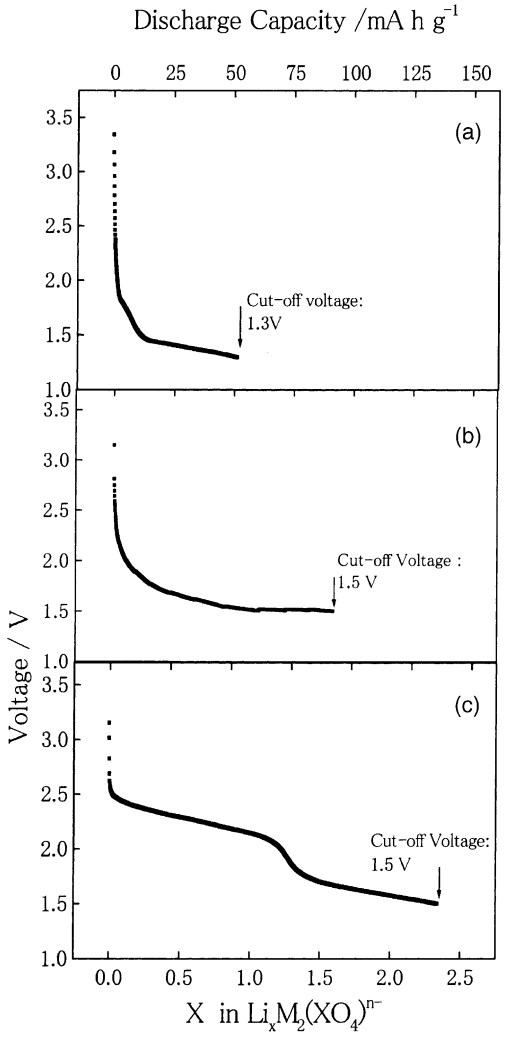

Fig. 3. Lithium intercalation into: (a) $Li_xCr_2(SO_4)_3$; (b) $Li_xCr_{0.5}Nb_{1.5}(SO_4)_3$; (c) $Li_xCr_{0.5}Nb_{1.5}(PO_4)_3$. Voltage profiles for the first discharge curve are shown.

change from sulfate to phosphate ion exhibits Nb^{5+}/Nb^{4+} and Nb^{4+}/Nb^{3+} redox couples, reflecting a shift in the energy of the redox couples through the decreased competition from the P atom for covalent mixing with oxygen. The weaker the competition, the stronger the covalent mixing at the given transition metal cations and the higher the energies of the redox couples. Unlike Nb^{5+}/Nb^{4+} and Nb^{4+}/Nb^{3+} redox couples in $(PO_4)^{3-}$, the Nb redox couples for $(SO_4)^{2-}$ are not distinct in the intercalation process. Polyanion influences the position of the redox potential of the Nb^{5+}/Nb^{4+} redox couple. Another difference in the electrochemical properties of the $(PO_4)^{3-}$ framework as compared to those of $(SO_4)^{2-}$ is the gain in the discharge capacity at the same cut-off voltage of 1.5 V. A discharge capacity of 142 mAh/g is observed in Fig. 3 for $(PO_4)^{3-}$, while it is 90 mAh/g for the $(SO_4)^{2-}$ framework. This may be due to the presence of phosphate polyanions in the structure, which tunes the Nb^{5+}/Nb^{4+} redox couple at 2.3 V, whereas in sulfate, the redox couple Nb^{5+}/Nb^{4+} is absent. Phosphate

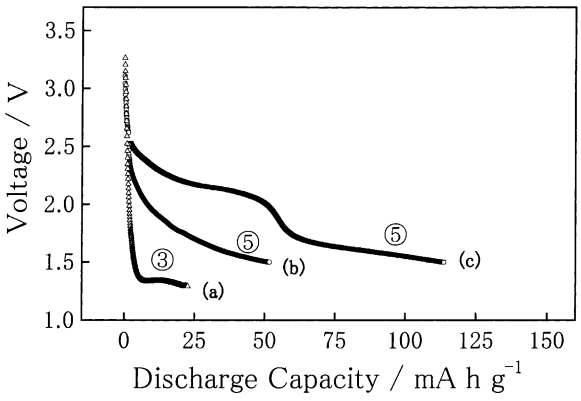

Fig. 4. Cycling behavior of the cell over subsequent cycles: (a) $Li_xCr_2(SO_4)_3$; (b) $Li_xCr_{0.5}Nb_{1.5}(SO_4)_3$; (c) $Li_xCr_{0.5}Nb_{1.5}(PO_4)_3$.

and sulfur have dissimilar characteristics in terms of their roles in tuning the redox couple.

Fig. 4 shows the cycling performance in terms of voltage obtained between 3.2 and 1.5 V for Nb-substituted polyanion and between 3.2 and 1.3 V for $Li|Li_xCr_2(SO_4)_3$ versus discharge capacity for this series of polyanions. The available capacity decreases for the $(SO_4)^{2-}$ electrodes. However, electrodes with Nb-substituted $(SO_4)^{2-}$ show significantly improved capacity retention during cycling, although this is still less than that of $(PO_4)^{3-}$. For example, $Li|Li_xCr_{0.5}Nb_{1.5}(PO_4)_3$ cells show an initial capacity of 142 mAh/g that decreases to 117 mAh/g after five cycles, reflecting a 16% loss, whereas $Li|Li_xCr_{0.5}Nb_{1.5}(SO_4)_3$ cells show an initial capacity of 90 mAh/g that decreases to 50 mAh/g over the same number of cycles (50% loss). $(PO_4)^{3-}$ electrodes are tested and are found to be capable of repeated cycling. Apparently, the Nb-substituted samples were more tolerant to repeated lithium insertion and extraction than $Li_xCr_2(SO_4)_3$ and the capacity was improved by substituting $(PO_4)^{3-}$ for $(SO_4)^{2-}$.

Fig. 5 shows open-circuit voltage for $A_xM_2(XO_4)^{n-}$ polyanions. The open-circuit voltage (V_{oc}) curve of an electrochemical cell provides information on the behavior of the cell under the condition of zero current flow. V_{oc} of the

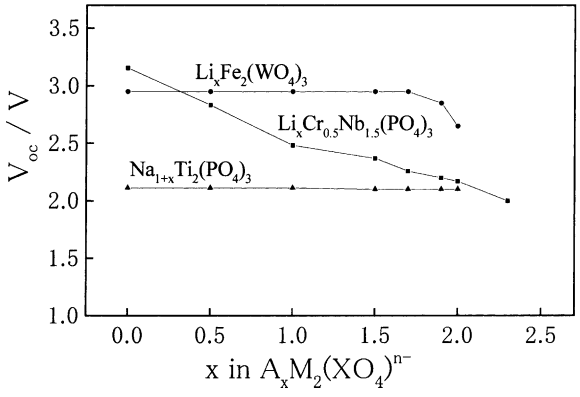

Fig. 5. Open-circuit voltage (V_{oc}) for various $A_xM_2(XO_4)^{n-}$ cells. $Li_xFe_2(WO_4)_3$ data from [18] and $Na_{1+x}Ti_2(PO_4)_3$ data from [8].

$Li|Li_xCr_{0.5}Nb_{1.5}(PO_4)_3$ cell as a function of x ($0 \leq x \leq 2.3$) in Fig. 5 as measured as follows: the cell was first discharged to a desired x (say, $x = 0.5$) and then left on open circuit (zero current flow) for 5 h. The final cell voltage was recorded as the V_{oc} for that composition. The V_{oc} of this cell is compared with those of various prototype intercalation compounds with the $A_xM_2(XO_4)^{n-}$ polyanion structure: $Li_3Fe_2(WO_4)_3$ from [18] and $Na_{1+x}Ti_2(PO_4)_3$ data from [8]. The open-circuit voltage (V_{oc}) versus lithium content for $Li|Li_xFe_2(WO_4)_3$ shows a plateau in the region of $0 < x < 1.7$, which substantiates the two-phase monoclinic framework in this range and the orthorhombic phase over the compositional range of $1.7 < x \leq 2.0$. Substitution of the polyanion with X = P, and sodium as the intercalation compound, $Na|Na_{1+x}Ti_2(PO_4)_3$, also showed a two-phase mechanism. These types of reactions are termed topotactic because they involve a phase transition in which a substantial structural change occurs, thereby affecting the long-term cycling of cell [19]. In contrast, the hexagonal $Li_xCr_{0.5}Nb_{1.5}(PO_4)_3$ as a cathode with cut-off voltages between 3.2 and 1.5 V shows a gradual downward sloping curve instead of a flat one while at least two lithium atoms per formula unit are inserted electrochemically in the first discharge cycle. The potential on the discharge curve gradually decreases downward and is not flat; this is indicative of the retention of the hexagonal framework over the entire region of the reaction. Thus, a single-phase region that allows the reaction to be reversible and capable of long life cycling is essential.

4. Conclusions

The $Cr_2(SO_4)_3$ framework described in this paper showed interesting electrochemical properties that depend on the substituted cation and the nature of the polyanion. The intercalation of lithium into $(XO_4)^{n-}$ polyanion, corresponding to the reduction of Nb^{5+}/Nb^{4+} redox potential at 2.3 V and Nb^{4+}/Nb^{3+} at 1.7 V versus lithium was determined. The open-circuit voltage was nearly independent of the nature of the polyanion but there was a decrease of 0.2 V for the cation substitution. A clear dependence of: (i) the shape of the discharge curve versus capacity; and (ii) the discharge capacity on the substituted Nb and the nature of the polyanion of the cathode material was obtained. Among the materials studied, $Li_xCr_{0.5}Nb_{1.5}(PO_4)_3$ showed that the reversible intercalation of lithium can be achieved electrochemically via a single-phase behavior over the entire region and this material is capable of repeated cycling. Cyclic performance was improved by the substitution of Nb for Cr, and this can be explained by the fact that Nb cations enhance the stability of the octahedral sites in the structure. The $(XO_4)^{n-}$ polyanions not only formed framework structures that supported fast Li^+ ion conduction, but also introduced a redox potential that gave technically attractive battery voltages for Nb and Cr.

Acknowledgements

One of the authors (Manickam) wishes to acknowledge the financial support, in the form of an award of Monbusho fellowship by Ministry of Education, Science, Sports and Culture of Japan.

References

[1] J.M. Tarascon, W.R. McKinnon, F. Coowar, T.N. Boowmer, G. Amatucci, D. Guyomard, J. Electrochem. Soc. 141 (1994) 1421.
[2] T. Ohzuku, M. Kitagawa, T. Hirai, J. Electrochem. Soc. 137 (1990) 769.
[3] K. Mizushima, P.C. Jones, P.J. Wiseman, J.B. Goodenough, Mater. Res. Bull. 15 (1980) 783.
[4] E. Plichta, M. Salomon, S. Slane, M. Uchiyama, D. Chua, W.B. Ebner, H.W. Lin, J. Power Sources 21 (1987) 25.
[5] W.M. Reiff, J.H. Zhang, C.C. Torardi, J. Solid State Chem. 62 (1986) 231.
[6] C.C. Torardi, E. Prince, Mater. Res. Bull. 21 (1986) 719.
[7] M.H. Rapposch, J.B. Anderson, E. Kostiner, Inorg. Chem. 19 (1980) 3531 and references cited therein.
[8] C. Delmas, F. Cherkaoui, A. Nadiri, P. Hagenmuller, Mater. Res. Bull. 22 (1987) 631.
[9] T. Oota, I. Yamai, J. Am. Ceram. Soc. 69 (1986) 1.
[10] H.Y.-P. Hong, Mater. Res. Bull. 11 (1976) 173.
[11] A.B. Bykov et al., Solid State Ion. 38 (1990) 31.
[12] G.V. SubbaRao, U.V. Varadaraju, K. Thomas, B. Sivasankar, J. Solid State Chem. 70 (1987) 101.
[13] M. Manickam, K. Ishibashi, M. Takata, in: Proceedings of the 11th Fall Meet, The Ceramics Society of Japan, Nagoya, 1998, p. 3.
[14] M. Manickam, K. Ishibashi, M. Takata, in: Proceedings of the Electrochemical Society of Japan, Nagaoka, 1998, p. 1.
[15] JCPDS card: $Cr_2(SO_4)_3$, 31-414.
[16] M.S. Whittingham, Intercalation Chemistry, Academic Press, New York, 1982, p. 274, 581.
[17] A. Mbandza, E. Bordes, P. Courtine, Mater. Res. Bull. 20 (1985) 251.
[18] A. Manthiram, J.B. Good Enough, J. Solid State Chem. 71 (1987) 349.
[19] M.S. Whittingham, MRS Bull. 25 (2000) 39.